Joint Trajectory and Resource Optimization for RIS Assisted UAV Cognitive Radio

Yingfeng Yu, Xin Liu, *Senior Member, IEEE,* Zechen Liu, and Tariq S Durrani, *Life Fellow, IEEE*

***Abstract*—Unmanned ariel vehicle (UAV) can be used in cognitive radio (CR) due to its high mobility and line-of-sight (LoS) transmission. However, the throughput of secondary user (SU) may decrease because of interference arising from spectrum sharing. Reconfigurable intelligent surface (RIS) may overcome the interference by reconstructing the propagation links. Our aim is to maximize the throughput of SU subject to the interference constraint of primary user (PU) through the joint optimization of the UAV's trajectory, RIS's passive beamforming and UAV's power allocation. We divide the formulated non-convex optimization problem into three subproblems: passive beamforming optimization, power allocation optimization and trajectory design, and then propose an alternating iterative optimization algorithm of the subproblems to get the suboptimal solutions. Numerical results show the proposed algorithm can achieve remarkable throughput gain.**

***Index Terms*—UAV, RIS, CR, trajectory optimization, throughput.**

I. Introduction

Possessing the advantages of low cost, fast mobility and high flexibility, unmanned ariel vehicle (UAV) is playing a critical role in wireless communications to assist the information transmissions. It can perform as an ariel base station (BS), relay or accessing point on account of its larger coverage and light-of-sight (LoS) transmission [1]–[3]. However, the UAV-enabled high-frequency communications often encounter spectrum scarcity. Cognitive radio (CR) technology can be applied to relieve such problem by making UAV dynamically access the spectrum bands licensed to primary users (PUs) for serving secondary users (SUs). [4] exploited the UAV as the BS of CR network and maximized its average secrecy rate via optimizing the trajectory and transmit power of UAV. [5] maximized the throughput of UAV enabled CR subject to preventing the interference with the PUs and meeting the throughput requirement of SUs.

However, the LoS links for UAV enabled CR are not always available due to blockages of high buildings. Fortunately, reconfigurable intelligent surface (RIS) is helpful to enhance the power of the UAV's signal in fading channels. To maximize the transmission gain, the RIS deploys a lot of passive elements to intelligently adjust the reflecting coefficients of the incident signals. [6] maximized the achievable rate of SU in an RIS-aided CR by jointly optimizing power allocation of SBs and passive beamforming of RIS. [7] proposed an RIS-assisted multiple-input multiple-output (MIMO) CR system and maximized its achievable sum rate through the optimization of the the transmit precoding, the power allocation of the SBS and the phase shifts of the RIS. In [8], the authors proposed the RIS-enabled CRN with NOMA and maximized both the spectrum efficiency and energy efficiency.

The existing studies usually consider UAV or RIS assisted CR independently, but a single UAV link or RIS link may be blocked by high buildings. Although [9] integrates UAV and RIS into CR, but it assumes a fixed UAV to serve SUs without considering UAV mobility and also ignores the effect of RIS on PU. In this paper, we assume that both SU and PU can benefit from RIS, and the SU can achieve better communication links and resist the interference with PU by exploring both UAV mobility and RIS link configuration. The main contributions of this paper are listed as follows.

- We present an RIS assisted UAV CR model, where both the SU and PU can benefit from RIS in terms of spectrum sharing. By considering the interference between SU and PU, the average rate maximization problem is formulated by means of jointly optimizing RIS phase-shift coefficients, UAV power allocation and UAV's trajectory.
- We divide the formulated non-convex optimization problem into three subproblems. By fixing the other two factors, we use the semidefinite relaxation method to solve the RIS phase shifts optimization. Likewise, we optimize the UAV trajectory by the successive convex approximation (SCA) method and get the optimal UAV power allocation using the standard convex optimization. Finally, an alternating iterative optimization algorithm of the three subproblems is proposed to find its suboptimal solutions.

II. System Model

As shown in Fig. 1, we consider an RIS assisted UAV CR system constituting a PU, an SU, a PBS and a UAV serving as SBS. We assume that the direct links from PBS to PU and SBS to SU are all blocked, and thus the RIS is used to reflect the signals of PBS and SBS to PU and SU, respectively. The summary of notations in the paper is shown in Table I. We use 3-D Cartesian coordinate to give the positions of the PBS, PU, SU as $\boldsymbol{w}_B = \{x_b, y_b, z_b\}^T, \boldsymbol{w}_P = \{x_b, y_b, 0\}^T, \boldsymbol{w}_S = \{x_b, y_b, 0\}^T$, respectively. For simplicity, the UAV's flying time T is divided into K time slots with each one the same

Manuscript received xx, xxxx; revised August xx, xxxx. (*Correspondence author: Xin Liu*)

Y. F. Yu, X. Liu and Z. C. Liu are with the School of Information and Communication Engineering, Dalian University of Technology, Dalian 116024, China (e-mail: yyf99s@163.com; liuxinstar1984@dlut.edu.cn; lzc_sdzb@mail.dlut.edu.cn).

T. S. Durrani is with the Department of Electronic and Electrical Engineering, University of Strathclyde, Glasgow G1 1XQ, U.K. (e-mail: durrani@strath.ac.uk).

TABLE I: Summary of Notations

Notation	Meaning
P_{max}	maximum power of the SBS
P_{min}	minimum power of the SBS
P_{avg}	average power of the SBS
p_b	the transmit power of PBS
v_{max}	maximum velocity of UAV
T	total flying time
δ	length of time slot
χ	antenna separation
λ	carrier wavelength
β	pass loss exponent for direct link
τ	pass loss exponent for reflect link
σ^2	noise power
ε	convergence threshold
M	number of RIS elements
K	number of time slots

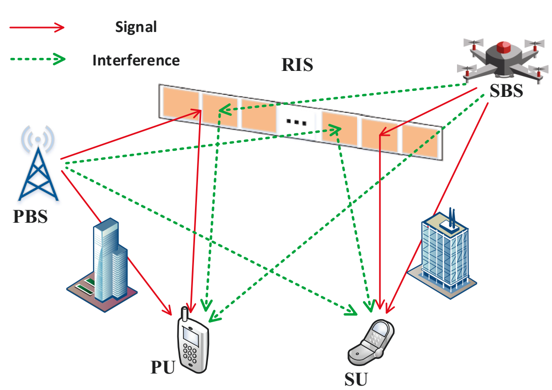

Fig. 1: RIS assisted UAV CR model.

lenghth $\delta = \frac{T}{K}$. The UAV moves in the x-y-z space and the maximum speed v_m. Hence, in slot k, the UAV's horizontal coordinate is denoted by $\boldsymbol{l}[k] = \{x_u[k], y_u[k], z_u[k]\}^T, k \in \mathcal{K} = \{1, 2, \ldots, K\}$. The following constraints should be met in terms of the positions of the UAV in two adjacent time slots

$$\|\boldsymbol{l}[k+1] - \boldsymbol{l}[k]\|^2 \leq D^2, k = 1, 2, \ldots, K-1, \tag{1a}$$
$$\|\boldsymbol{l}[1] - \boldsymbol{l}_0\|^2 \leq D^2, \tag{1b}$$
$$\|\boldsymbol{l}_F - \boldsymbol{l}[k]\|^2 \leq D^2, \tag{1c}$$
$$H_{min} \leqslant z_u[k] \leqslant H_{max}, \forall k, \tag{1d}$$

where $\boldsymbol{l}_0$ and $\boldsymbol{l}_F$ denote the UAV's starting and final locations, respectively, and the maximum traveling distance of the UAV within one time slot is $D = v_m \delta$.

The proper power allocation for the SBS will have a positive impact on the improvement of the CR system. $p[k]$ represents the transmit power of the UAV at the kth time slot, and the the following power constraints of the UAV should be satisfied

$$\frac{1}{K} \sum_{k \in \mathcal{K}} p[k] \leqslant P_{avg} \tag{2}$$

$$P_{min} \leqslant p[k] \leqslant P_{max}, k \in \mathcal{K}, \tag{3}$$

where P_{avg}, P_{max} and P_{min} represent UAV's average power, maximum power and minimum power for each time slot.

The RIS consisting of M passive elements forms a ULA, which the central controller can manipulate to intelligently adjust the incident signals. The diagonal phase-shift matrix can be expressed as $\boldsymbol{\Theta}[k] = \mathrm{diag}\{e^{j\theta_1[k]}, e^{j\theta_2[k]}, \ldots, e^{j\theta_M[k]}\}, k \in \mathcal{K}$, where $\theta_i[k]$ means the phase shift of the ith element at the kth time slot. We assume that the phase shift of each element can be continuously adjusted. And the RIS is vertically hung on a building at the position of $\boldsymbol{w}_R = \{x_r, y_r, z_r\}^T$.

Because the UAV flies at a high enough altitude, the link between the UAV and the RIS (U-R link) can be assumed as a LoS channel [10]. So the channel gain of the U-R link, denoted by $\boldsymbol{h}_{ur}[k]$, can be expressed by $\boldsymbol{h}_{ur}[k] = \sqrt{\rho d_{ur}^{-2}[k]} \tilde{\boldsymbol{h}}_{ur}[k]$, where $\tilde{\boldsymbol{h}}_{ur}[k] = \{1, e^{-j\frac{2\pi}{\lambda}\chi\phi_{ur}[k]}, \ldots, e^{-j\frac{2\pi}{\lambda}\chi(M-1)\phi_{ur}[k]}\}^{\mathrm{T}}$, ρ represents the path loss at the unit distance of $D_0 = 1$m, $d_{ur}[k]$ means the distance between the UAV and the RIS at the time slot, χ and λ represent the antenna separation and carrier wavelength, respectively, and $\phi_{ur}[k] = \frac{x_r - x_u[k]}{d_{ur}[k]}$.

We use the Rician fading channel to model the links from RIS to SU (R-S link), RIS to PU (R-P link), and PBS to RIS (B-R link)[11]. The corresponding channel gains of the three links are denoted by $\boldsymbol{h}_{rs}, \boldsymbol{h}_{rp}$ and $\boldsymbol{h}_{br}$, respectively. For example, $\boldsymbol{h}_{rs}$ can be expressed as $\boldsymbol{h}_{rs} = \sqrt{\rho d_{rs}^{-\tau}}\{\sqrt{\frac{\varepsilon}{1+\varepsilon}} \boldsymbol{h}_{rs}^{LoS} + \sqrt{\frac{1}{1+\varepsilon}} \boldsymbol{h}_{rs}^{nLoS}\}$, where τ denotes the path loss exponent of the links modeled by Rician fading channel, d_{rs} is the distance between the RIS and the SU, ε is the Rician factor, the LoS component $\boldsymbol{h}_{rs}^{LoS} = \{1, e^{-j\frac{2\pi}{\lambda}\chi\phi_{rs}}, \ldots, e^{-j\frac{2\pi}{\lambda}\chi(M-1)\phi_{rs}}\}^{\mathrm{T}}$, and $\phi_{rs} = \frac{x_s - x_r}{d_{rs}}$; $\boldsymbol{h}_{rs}^{nLoS} \in \mathbb{C}^{M \times 1}$ is the non-LoS (NLoS) component, which is independently drawn from the circularly symmetric complex Gaussian (CSCG) distribution with zero mean and unit variance.

Though the direct links from UAV to SU (U-S link), UAV to PU (U-P link), PBS to SU (B-S link) and PBS to PU (B-P link) are blocked, there still exist many scattered signals [11]. So they are modeled by the Rayleigh fading channel. The channel gains of the U-S link, U-P link and B-S link are denoted by h_{us}, h_{up}, h_{bs} and h_{bp}, respectively. For instance, h_{us} can be expressed as $h_{us}[k] = \sqrt{\rho d_{us}^{-\beta}[k]} \tilde{h}$, where β is the path loss exponent of the U-S link, $d_{us}[k]$ is the distance betwwen the UAV and the SU, and $\tilde{h}$ is the random scattering component modeled by zero-mean and unit-variance CSCG distribution.

To guarantee the communication performance of the PU, the interference from UAV to PU should be controlled as

$$\frac{1}{K} \sum_{k \in \mathcal{K}} p[k] |h_{up} + \boldsymbol{h}_{rp}^{\boldsymbol{H}} \boldsymbol{\Theta}[k] \boldsymbol{h}_{ur}[k]|^2 \leqslant P_t, \forall k \tag{4}$$

where P_t is the average maximum interference power the PU can tolerate per time slot. The throughput of the SU at each time slot can be expressed as

$$R[k] = \log_2(1 + \frac{p[k]|h_{us}[k] + \boldsymbol{h}_{rs}^{\boldsymbol{H}} \boldsymbol{\Theta}[k] \boldsymbol{h}_{ur}[k]|^2}{p_b |h_{bs} + \boldsymbol{h}_{rs}^{\boldsymbol{H}} \boldsymbol{\Theta}[k] \boldsymbol{h}_{br}|^2 + \sigma^2}) \tag{5}$$

where p_b is the transmit power of PBS and σ^2 denotes the additive while Gaussian noise. And the average throughput is $\bar{R} = \frac{1}{K}\sum_{k\in\mathcal{K}} R[k]$.

III. Problem Formulation

Our aim is to maximize the average rate $\bar{R}$ via the joint optimization of the UAV's power allocation $\boldsymbol{p} \triangleq \{p[k], k \in \mathcal{K}\}$, the RIS phase shifts $\boldsymbol{\Phi} \triangleq \{\boldsymbol{\Theta}[k], k \in \mathcal{K}\}$, and the UAV trajectory $\boldsymbol{L} \triangleq \{\boldsymbol{l}[k], k \in \mathcal{K}\}$. The problem is listed as follows

$$\max_{(\boldsymbol{p},\boldsymbol{\Phi},\boldsymbol{L})} \bar{R} \tag{6a}$$
$$s.t.\ 0 \leqslant \theta_i[k] < 2\pi, \forall i, k, \tag{6b}$$
$$\frac{1}{K}\sum_{k\in\mathcal{K}} p[k]|h_{up} + \boldsymbol{h}_{rp}^{\boldsymbol{H}}\boldsymbol{\Theta}[k]\boldsymbol{h}_{ur}[k]|^2 \leqslant P_t, \tag{6c}$$
$$\frac{1}{K}\sum_{k\in\mathcal{K}} p[k] \leqslant P_{avg} \tag{6d}$$
$$P_{min} \leqslant p[k] \leqslant P_{max}, \forall k \tag{6e}$$
$$(1a) - (1d) \tag{6f}$$

Owing to the non-convex objective function and the highly coupled variables $\boldsymbol{p}, \boldsymbol{\Phi}, \boldsymbol{L}$, the problem (6) fails to be a convex optimization problem. To make (6) tractable, we divide the original problem into separate subproblems and then use alternating optimization tool to get the approximately optimal solutions.

IV. Solution Algorithm

The originally formulated optimization problem will be separated into the following subproblems: RIS phase shifts, UAV's power allocation optimization and UAV's trajectory design. Moreover, we propose an alternating iterative optimization algorithm to obtain the approximately optimal solutions to (6).

A. UAV Power Allocation Optimization

When other two variables are given, the problem (6) can be expressed as

$$\max_{\boldsymbol{p}} \frac{1}{K}\sum_{k\in\mathcal{K}} \log_2(1 + p[k]\gamma_0[k]) \tag{7a}$$
$$s.t.\ \frac{1}{K}\sum_{k\in\mathcal{K}} p[k]|h_{up} + \boldsymbol{h}_{rp}^{\boldsymbol{H}}\boldsymbol{\Theta}[k]\boldsymbol{h}_{ur}[k]|^2 \leqslant P_t, \forall k \tag{7b}$$
$$\frac{1}{K}\sum_{k\in\mathcal{K}} p[k] \leqslant P_{avg} \tag{7c}$$
$$P_{min} \leqslant p[k] \leqslant P_{max}, \forall k, \tag{7d}$$

where $\gamma_0[k] = \frac{|h_{us}[k] + \boldsymbol{h}_{rs}^{\boldsymbol{H}}\boldsymbol{\Theta}[k]\boldsymbol{h}_{ur}[k]|^2}{p_b|h_{bs} + \boldsymbol{h}_{rs}^{\boldsymbol{H}}\boldsymbol{\Theta}[k]\boldsymbol{h}_{br}|^2 + \sigma^2}$ is a constant for each time slot. And the problem (7) is a standard convex optimization problem and can be solved by CVX.

B. RIS Phase Shift Optimization

Firstly, we let $\boldsymbol{g}_{us}[k] = \{\boldsymbol{h}_{rs}^{\boldsymbol{H}} diag\{\boldsymbol{h}_{ur}[k]\}, h_{us}[k]\}^{\mathrm{T}} \in \mathbb{C}^{M+1}$, $\boldsymbol{g}_{up}[k] = \{\boldsymbol{h}_{rp}^{\boldsymbol{H}} diag\{\boldsymbol{h}_{ur}[k]\}, h_{up}[k]\}^{\mathrm{T}} \in \mathbb{C}^{M+1}$, $\boldsymbol{g}_{bs} = \{\boldsymbol{h}_{rs}^{\boldsymbol{H}} diag\{\boldsymbol{h}_{br}\}, h_{bs}\}^{\mathrm{T}} \in \mathbb{C}^{M+1}$and $\boldsymbol{u}[k] = \{e^{j\theta_1[k]}, \ldots, e^{j\theta_i[k]}, \ldots, e^{j\theta_M[k]}, 1\}^{\mathrm{T}} \in \mathbb{C}^{M+1}$. Then, the expressions of the channel gains can be rewritten as

$$|h_{us}[k] + \boldsymbol{h}_{rs}^{\boldsymbol{H}}\boldsymbol{\Theta}[k]\boldsymbol{h}_{ur}[k]|^2 = \mathrm{Tr}\{\mathbf{H}_{us}[k]\mathbf{U}[k]\}, \forall k, \tag{8}$$
$$|h_{up}[k] + \boldsymbol{h}_{rp}^{\boldsymbol{H}}\boldsymbol{\Theta}[k]\boldsymbol{h}_{ur}[k]|^2 = \mathrm{Tr}\{\mathbf{H}_{up}[k]\mathbf{U}[k]\}, \forall k, \tag{9}$$
$$|h_{bs} + \boldsymbol{h}_{rs}^{\boldsymbol{H}}\boldsymbol{\Theta}[k]\boldsymbol{h}_{br}|^2 = \mathrm{Tr}\{\mathbf{H}_{bs}\mathbf{U}[k]\}, \forall k, \tag{10}$$

where $\mathbf{H}_{us}[k] = \boldsymbol{g}_{us}[k]\boldsymbol{g}_{us}^{\mathrm{H}}[k]$, $\mathbf{H}_{up}[k] = \boldsymbol{g}_{up}[k]\boldsymbol{g}_{up}^{\mathrm{H}}[k]$, $\mathbf{H}_{bs} = \boldsymbol{g}_{bs}\boldsymbol{g}_{bs}^{\mathrm{H}}$, $\mathbf{U}[k] = \boldsymbol{u}[k]\boldsymbol{u}^{\mathrm{H}}[k]$ and $\mathrm{Tr}\{\mathbf{A}\}$ means the trace of the matrix $\mathbf{A}$. We then introduce slack variables $\boldsymbol{\xi} \triangleq \{\xi[k], k \in \mathcal{K}\}$ and $\boldsymbol{\zeta} \triangleq \{\zeta[k], k \in \mathcal{K}\}$ to slack the SNR and the total noise power of the SU at each time slot. Hence, the problem (6) can be reformulated as

$$\max_{(\mathbf{U},\boldsymbol{\xi},\boldsymbol{\zeta})} \frac{1}{K}\sum_{k\in\mathcal{K}} \log_2(1 + \xi[k]) \tag{11a}$$
$$s.t.\ p[k]\mathrm{Tr}\{\mathbf{H}_{us}[k]\mathbf{U}[k]\} \geqslant \xi[k]\zeta[k], \forall k, \tag{11b}$$
$$\zeta[k] \geqslant p_b\mathrm{Tr}\{\mathbf{H}_{bs}\mathbf{U}[k]\} + \sigma^2, \forall k, \tag{11c}$$
$$\frac{1}{K}\sum_{k\in\mathcal{K}} p[k]\mathrm{Tr}\{\mathbf{H}_{up}[k]\mathbf{U}[k]\} \leqslant P_t, \tag{11d}$$
$$\mathbf{U}[k] \succeq 0, \forall k, \tag{11e}$$
$$\mathbf{U}_{(i,i)}[k] = 1, \forall k, i = 1, 2, \ldots, M+1 \tag{11f}$$
$$rank\{\mathbf{U}[k]\} = 1, \forall k, \tag{11g}$$

where $rank\{\mathbf{A}\}$ means the rank of matrix $\mathbf{A}$. However, the variables $\boldsymbol{\xi}$ and $\boldsymbol{\zeta}$ in the constraint (11b) is highly coupled. Therefore, we use Taylor expansion to expand $\xi[k]\zeta[k]$ at the feasible point $\boldsymbol{\xi}_0 = \{\xi_0[k]\}_{k=1}^{K}$ and $\boldsymbol{\zeta}_0 = \{\zeta_0[k]\}_{k=1}^{K}$ like [8].

$$\begin{aligned}\xi[k]\zeta[k] \geqslant \xi_0[k]\zeta_0[k] + \zeta_0[k](\xi[k] - \xi_0[k])\\ + \xi_0[k](\zeta[k] - \zeta_0[k]) = \check{f}(\xi, \zeta), \forall k\end{aligned} \tag{12}$$

Moreover, since the rank one demand is always hard to satisfy, the semidefinite relaxation (SDR) method is applied. The problem (11) can be further reformulated as

$$\max_{(\mathbf{U},\boldsymbol{\xi},\boldsymbol{\zeta})} \frac{1}{K}\sum_{k\in\mathcal{K}} \log_2(1 + \xi[k]) \tag{13a}$$
$$s.t.\ p[k]\mathrm{Tr}\{\mathbf{H}_{us}[k]\mathbf{U}[k]\} \geqslant \check{f}(\xi, \zeta), \forall k, \tag{13b}$$
$$\zeta[k] \geqslant p_b\mathrm{Tr}\{\mathbf{H}_{bs}\mathbf{U}[k]\} + \sigma^2, \forall k, \tag{13c}$$
$$\frac{1}{K}\sum_{k\in\mathcal{K}} p[k]\mathrm{Tr}\{\mathbf{H}_{up}[k]\mathbf{U}[k]\} \leqslant P_t, \tag{13d}$$
$$\mathbf{U}[k] \succeq 0, \forall k, \tag{13e}$$
$$\mathbf{U}_{(i,i)}[k] = 1, \forall k, i = 1, 2, \ldots, M+1 \tag{13f}$$

which is concvx and can be solved by CVX. However, the optimization result usually cannot satisfy the rank one demand, and we need to recover it like [12].

C. UAV Trajectory Design

For the UAV CR, the trajectory design plays a quite significant role. For simplicity, we use the trajectory obtained from the last iteration to make ϕ_{ur}, ϕ_{rs} etc. known like [13]. We transform the expressions of the channel gains for the U-S link as follows with other two factors are fixed

$$\mu_{s1} = real(\sqrt{\rho}\tilde{h}),\ \nu_{s1} = imag(\sqrt{\rho}\tilde{h}), \tag{14}$$

$$\mu_{s2}[k] = real(\sqrt{\rho}\boldsymbol{h}_{rs}^{\boldsymbol{H}}\boldsymbol{\Theta}[k]\tilde{\boldsymbol{h}}_{ur}[k]), \forall k, \tag{15}$$

$$\nu_{s2}[k] = imag(\sqrt{\rho}\boldsymbol{h}_{rs}^{\boldsymbol{H}}\boldsymbol{\Theta}[k]\tilde{\boldsymbol{h}}_{ur}[k]), \forall k, \tag{16}$$

where μ_{s1} and ν_{s1} denote the real and imaginary parts of direct channel gain for U-S link, respectively, while μ_{s2} and ν_{s2} denote the real part and imaginary part of reflecting channel gain for U-S link, respectively. Then we process the channel gains of U-P link as the U-S link, and the corresponding parts are denoted by $\nu_{p1}, \mu_{p1}, \nu_{p2}[k], \mu_{p2}[k]$. Hence, the problem (6) can be reformulated as

$$\max_{(\boldsymbol{L})} \bar{R} \tag{17a}$$

$$s.t.\ \frac{1}{K}\sum_{k\in\boldsymbol{\mathcal{K}}} p[k](\frac{\omega_{p1}}{d_{up}^{\beta}[k]} + \frac{\omega_{p2}[k]}{d_{ur}^{2}[k]} + \frac{\omega_{p3}[k]}{d_{up}^{\frac{\beta}{2}}[k]d_{ur}[k]}) \leqslant P_t \tag{17b}$$

$$(1a) - (1c) \tag{17c}$$

where ω_{s1}, $\omega_{s2}[k]$, $\omega_{s3}[k]$, ω_{p1}, $\omega_{p2}[k]$ and $\omega_{p3}[k]$ are given in (18) and (19) at the top of the next page, and $\bar{R}$ is given as

$$\bar{R} = \frac{1}{K}\sum_{k\in\boldsymbol{\mathcal{K}}} \log_2(1+\gamma_0[k](\frac{\omega_{s1}}{d_{us}^{\beta}[k]} + \frac{\omega_{s2}[k]}{d_{ur}^{2}[k]} + \frac{\omega_{s3}[k]}{d_{us}^{\frac{\beta}{2}}[k]d_{ur}[k]})),$$

where $\gamma_0[k] = \frac{p[k]}{p_b|h_{bs}+\boldsymbol{h}_{rs}^{\boldsymbol{H}}\boldsymbol{\Theta}[k]\boldsymbol{h}_{br}|^2+\sigma^2}, \forall k$ is a constant.

But still, the problem (17) is a non-convex optimization problem in respect of the UAV's trajectory $\boldsymbol{L}$. Then, introducing some slack variables $\boldsymbol{c} \triangleq \{c[k]\}$, $\boldsymbol{e} \triangleq \{e[k]\}$,$\boldsymbol{n} \triangleq \{n[k]\}$ and $\boldsymbol{s} \triangleq \{s[k]\}, k \in \boldsymbol{\mathcal{K}}$, the problem (17) is rewritten as

$$\max_{\substack{(\boldsymbol{L},\boldsymbol{c},\\ \boldsymbol{e},\boldsymbol{n},\boldsymbol{s})}} \frac{1}{K}\sum_{k\in\boldsymbol{\mathcal{K}}} \log_2(1+\gamma_0[k](\frac{\omega_{s1}}{c^{\beta}[k]} + \frac{\omega_{s2}[k]}{e^{2}[k]} + \frac{\omega_{s3}[k]}{c^{\frac{\beta}{2}}[k]e[k]})) \tag{20a}$$

$$s.t.\ \frac{1}{K}\sum_{k\in\boldsymbol{\mathcal{K}}} p[k](\frac{\omega_{p1}}{n^{\beta}[k]} + \frac{\omega_{p2}[k]}{s^{2}[k]} + \frac{\omega_{p3}[k]}{n^{\frac{\beta}{2}}[k]s[k]}) \leqslant P_t \tag{20b}$$

$$c[k] \geqslant d_{us}[k], \forall k, \tag{20c}$$

$$e[k] \geqslant d_{ur}[k], \forall k, \tag{20d}$$

$$n[k] \leqslant d_{up}[k], \forall k, \tag{20e}$$

$$s[k] \leqslant d_{ur}[k], \forall k, \tag{20f}$$

$$(1a) - (1d) \tag{20g}$$

The problems (17) and (20) are equivalent if (20c), (20d), (20e) and (20f) hold equality. Otherwise, the increase of $\boldsymbol{u}$ and $\boldsymbol{v}$ will decrease the objective value, and the decrease of $\boldsymbol{n}$ and $\boldsymbol{s}$ will probably not satisfy the constraint (20b). According to the Lemma in [14], we can process the objective value likewise by Taylor Expansion at the feasible points $\boldsymbol{c}_0 = \{c_0[k]\}_{k=1}^{K}$, $\boldsymbol{e}_0 = \{e_0[k]\}_{k=1}^{K}$, $\boldsymbol{n}_0 = \{n_0[k]\}_{k=1}^{K}$,$\boldsymbol{s}_0 = \{s_0[k]\}_{k=1}^{K}$ and $\mathbf{L}_0 = \{\boldsymbol{l}_0[k]\}_{k=1}^{K}$. The constraints are converted to convex as

$$\log_2(1+\gamma_0[k](\frac{\omega_{s1}}{c^{\beta}[k]} + \frac{\omega_{s2}[k]}{e^{2}[k]} + \frac{\omega_{s3}[k]}{c^{\frac{\beta}{2}}[k]e[k]})) \geqslant \log_2(A_{s0}[k]) + B_{s0}[k](c[k]-c_0[k]) + C_{s0}[k](e[k]-e_0[k]) \tag{21}$$

$$\frac{\omega_{p1}}{n^{\beta}[k]} + \frac{\omega_{p2}[k]}{s^{2}[k]} + \frac{\omega_{p3}[k]}{n^{\frac{\beta}{2}}[k]s[k]} \geqslant A_{p0}[k] + B_{p0}[k](n[k]-n_0[k]) + C_{s0}[k](s[k]-s_0[k]), \forall k \tag{22}$$

$$c^2[k] \geqslant -c_0^2[k] + 2c_0[k]c[k], \forall k \tag{23}$$

$$e^2[k] \geqslant -e_0^2[k] + 2e_0[k]e[k], \forall k \tag{24}$$

$$d_{up}^2[k] \geqslant \|\boldsymbol{l}_0[k]-\boldsymbol{w}_p\|^2 + 2\|\boldsymbol{l}_0[k]-\boldsymbol{w}_p\|^T\|\boldsymbol{l}[k]-\boldsymbol{w}_p\|, \forall k \tag{25}$$

$$d_{ur}^2[k] \geqslant \|\boldsymbol{l}_0[k]-\boldsymbol{w}_r\|^2 + 2\|\boldsymbol{l}_0[k]-\boldsymbol{w}_r\|^T\|\boldsymbol{l}[k]-\boldsymbol{w}_r\|, \forall k \tag{26}$$

where $A_{s0}[k]$, $B_{s0}[k]$, $C_{s0}[k]$, A_{p0}, $B_{p0}[k]$, $C_{p0}[k]$ are

$$A_{s0}[k] = 1 + \gamma_0[k](\frac{\omega_{s1}}{c_0^{\beta}[k]} + \frac{\omega_{s2}[k]}{e_0^{2}[k]} + \frac{\omega_{s3}[k]}{c_0^{\frac{\beta}{2}}[k]e_0[k]}), \forall k \tag{27}$$

$$B_{s0}[k] = -\frac{\beta\gamma_0[k]}{A_{s0}\ln 2}[\frac{\beta\omega_{s1}}{c_0^{(\beta+1)}[k]} + \frac{\omega_{s3}}{2c_0^{(\beta/2+1)}[k]e_0[k]}], \forall k \tag{28}$$

$$C_{s0}[k] = -\frac{2\gamma_0[k]}{A_{s0}\ln 2}[\frac{2\omega_{s2}}{e_0^{3}[k]} + \frac{\omega_{s3}}{2c_0^{(\beta/2)}[k]e_0^{2}[k]}], \forall k \tag{29}$$

$$A_{p0}[k] = \frac{\omega_{s1}}{n_0^{\beta}[k]} + \frac{\omega_{s2}[k]}{s_0^{2}[k]} + \frac{\omega_{s3}[k]}{n_0^{\frac{\beta}{2}}[k]s_0[k]}, \forall k \tag{30}$$

$$B_{p0}[k] = -\beta[\frac{\beta\omega_{p1}}{n_0^{(\beta+1)}[k]} + \frac{\omega_{p3}}{2n_0^{(\beta/2+1)}[k]s_0[k]}], \forall k \tag{31}$$

$$C_{p0}[k] = -2[\frac{2\omega_{s2}}{s_0^{3}[k]} + \frac{\omega_{s3}}{2n_0^{(\beta/2)}[k]s_0^{2}[k]}], \forall k \tag{32}$$

Hereby, we can rewrite (20) as follows

$$\max_{(\boldsymbol{L},\boldsymbol{c},\boldsymbol{e},\boldsymbol{n},\boldsymbol{s})} \frac{1}{K}\sum_{k\in\boldsymbol{\mathcal{K}}} B_{s0}[k]c[k] + C_{s0}[k]e[k] \tag{33a}$$

$$s.t.\ \frac{p[k]}{N}\sum_{k\in\boldsymbol{\mathcal{K}}}(A_{p0} + B_{p0}[k](n[k]-n_0[k]) + C_{s0}[k](s[k]-s_0[k])) \leqslant P_t \tag{33b}$$

$$d_{us}^2[k] + c_0^2[k] - 2c_0[k]c[k] \leqslant 0, \forall k, \tag{33c}$$

$$d_{ur}^2[k] + e_0^2[k] - 2e_0[k]e[k] \leqslant 0, \forall k, \tag{33d}$$

$$n^2[k] \leqslant \|\boldsymbol{l}_0[k]-\boldsymbol{w}_p\|^2 + 2\|\boldsymbol{l}_0[k]-\boldsymbol{w}_p\|^T\|\boldsymbol{l}[k]-\boldsymbol{w}_p\|, \forall k, \tag{33e}$$

$$s^2[k] \leqslant \|\boldsymbol{l}_0[k]-\boldsymbol{w}_r\|^2 + 2\|\boldsymbol{l}_0[k]-\boldsymbol{w}_r\|^T\|\boldsymbol{l}[k]-\boldsymbol{w}_r\|, \forall k, \tag{33f}$$

$$(1a) - (1d) \tag{33g}$$

which is a convex optimization problem and can be addressed using CVX.

D. Alternating Iterative Optimization Algorithm

According to the above discussions, an alternating iterative optimization algorithm is proposed in Algorithm 1 to solve the original problem (6). Following the result in [15], the objective value $\bar{R}$ is guaranteed to increase and then converge over the iterations due to that there exists a boundary for the system throughput. The complexity of Algorithm 1 is calculated by $\mathcal{O}(C_{itr}(K^{3.5} + K(M+1)^{4.5} + (5K)^{3.5}))$, where C_{itr} is the

$$\omega_{s1}=\mu_{s1}^2+\nu_{s1}^2,\omega_{s2}[k]=\mu_{s2}^2[k]+\nu_{s2}^2[k],\omega_{s3}[k]=2\mu_{s1}\mu_{s2}[k]+2\nu_{s1}\nu_{s2}[k], \tag{18}$$

$$\omega_{p1}=\mu_{p1}^2+\nu_{p1}^2,\omega_{p2}[k]=\mu_{p2}^2[k]+\nu_{p2}^2[k],\omega_{p3}[k]=2\mu_{p1}\mu_{p2}[k]+2\nu_{p1}\nu_{p2}[k] \tag{19}$$

iteration number .

V. Numerical Results

The simulation parameters are set as follows. The Cartesian coordinates of each node are $\boldsymbol{w}_B=\{-500,200,10\}^T,\boldsymbol{w}_P=\{-150,160,0\}^T,\boldsymbol{w}_S=\{0,100,0\},\boldsymbol{w}_R=\{0,0,40\}^T$, respectively. The initial and ending coordinates of the UAV are (-500,20,80) and (500,20,80), respectively. The maximum velocity of the UAV is 25m/s. The path loss at D_0 = 1m is -20dB. And the rest of the parameters are H_{min} = 70m, H_{max} = 80m, δ = 1s, T = 100s, σ^2 = -80dBm, P_t = -70dBm, $\chi=\frac{\lambda}{2}$, $\alpha=2.8$, $\beta=2.5$, ε = 3dB, $K=100$, $P_b=100$mW, $P_{avg}=500$mW, $P_{min}=100$mW, $P_{max}=1000$mW.

Algorithm 1 Alternating iterative optimization for solving (6).

Initialize: the iteration number $j=0$, $\{\mathbf{L}^{[j]}$, $\mathbf{\Phi}^{[j]}$, $\boldsymbol{p}^{[j]}$, $\boldsymbol{c}^{[j]}$, $\boldsymbol{e}^{[j]}$, $\boldsymbol{n}^{[j]}$, $\boldsymbol{s}^{[j]}\}$, the average throughput $\bar{R}^{[j]}$ with the given variables;
1: **while** $\bar{R}$ is not convergent **do**
2: update $\mathbf{\Phi}^{[j+1]}$ via the solution of problem (13);
3: update $\mathbf{L}^{[j+1]}$, $\boldsymbol{c}^{[j+1]}$, $\boldsymbol{e}^{[j+1]}$, $\boldsymbol{n}^{[j+1]}$, $\boldsymbol{s}^{[j+1]}$ via the solution of problem (33);
4: update $\boldsymbol{p}^{[j+1]}$ via the solution of problem (7);
5: calculate $\bar{R}^{[j+1]}$, and set $j=j+1$;
6: **end while**
Output: the optimal solutions $\mathbf{L}^{[j]},\mathbf{\Phi}^{[j]},\boldsymbol{p}^{[j]}$.

Fig. 2 illustrates the optimized UAV trajectory, where the UAV flies to the best position close to the RIS and hovers at the minimum height of 70m for most of the time, in order to improve the RIS link gain. During coming to and leaving the hovering position, the UAV chooses to approach near the SU to improve the direct link gain. For the final iteration of the trajectory, since the UAV is far enough away from the PU, the interference of the UAV to the PU via the direct link is very weak. In addition, the RIS link can be adjusted to both improve the communication performance of the SU and control the interference to the PU.

Fig. 3 illustrates the optimized UAV power allocation. we can see that the majority of the power is allocated for the hovering time to improve the throughput of RIS link. For the coming and leaving time, only the minimum power is allocated to guarantee that the UAV can communicate with the SU during the whole flying time.

Fig. 4 demonstrates the comparison between our scheme with M = 30 and M = 35 and the following traditional UAV schemes with respect to the maximized rate of SU. **Our scheme (i)**: The proposed optimization scheme with M = 30. **Our scheme (ii)**: The proposed optimization scheme with M = 35. **Scheme (i)**: From starting point, the UAV travels directly to the final point with the fixed height (70m) and RIS ($M=30$). **Scheme (ii)**: The UAV trajectory is optimized

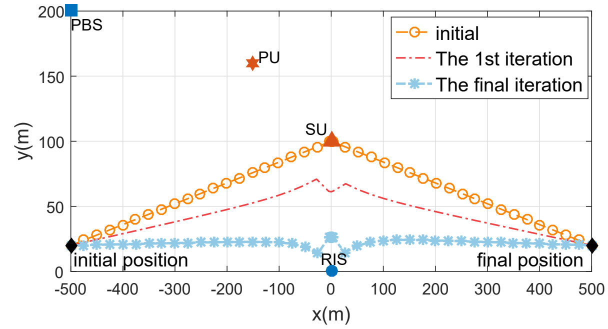

(a)

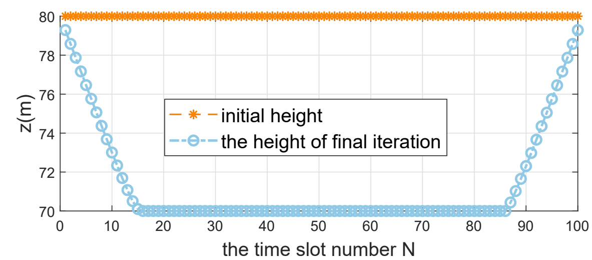

(b)

Fig. 2: The optimized trajectory: (a) the trajectory in x-y plain; (b) the height of the UAV.

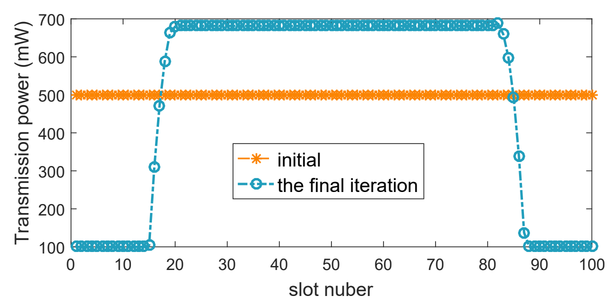

Fig. 3: The optimized UAV power allocation when $M=30$.

without RIS ($M=0$). **Scheme (iii)**: The UAV trajectory is optimized in x-y plane with the fixed height (70m) and RIS ($M=30$). Fig. 4 shows that the SU's rate improves when the number of RIS elements M increase because there exist more relaying channels. It is also seen that higher throughput gain can be achieved by our proposed scheme when compared with Scheme (i) through designing the UAV's trajectory.

VI. Conclusion

In this letter, we consider an RIS assisted UAV CR system, where we maximize the SU's throughout subject to the constraint of the interference with the PU by the joint optimization of RIS phase shift coefficients, UAV's trajectory and UAV power allocation. In order to tackle the non-convexity of the

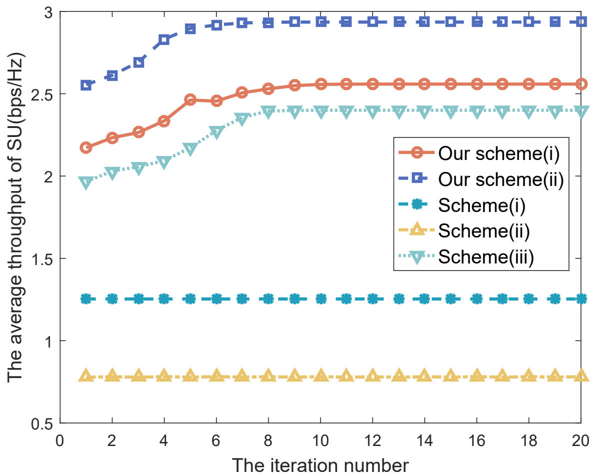

Fig. 4: Rate comparison between different schemes.

original problem, we divide the problem into three separate subproblems. Based on the solutions to each subproblem, we propose an alternating iterative optimization algorithm to obtain the approximately optimal solutions. Simulation results show the significant throughput gain when comparing our proposed scheme to other schemes.

References

[1] X. Li, H. Yao, J. Wang, X. Xu, C. Jiang, and L. Hanzo, "A near-optimal UAV-aided radio coverage strategy for dense urban areas," *IEEE Transactions on Vehicular Technology*, vol. 68, no. 9, pp. 9098–9109, 2019.

[2] J. Wang, C. Jiang, Z. Wei, C. Pan, H. Zhang, and Y. Ren, "Joint UAV hovering altitude and power control for space-air-ground iot networks," *IEEE Internet of Things Journal*, vol. 6, no. 2, pp. 1741–1753, 2019.

[3] C. Yan, L. Fu, J. Zhang, and J. Wang, "A comprehensive survey on UAV communication channel modeling," *IEEE Access*, vol. 7, pp. 107 769–107 792, 2019.

[4] Y. Zhou, F. Zhou, H. Zhou, D. W. K. Ng, and R. Q. Hu, "Robust trajectory and transmit power optimization for secure UAV-enabled cognitive radio networks," *IEEE Trans. Commun.*, vol. 68, no. 7, pp. 4022–4034, 2020.

[5] S. K. Nobar, M. H. Ahmed, Y. Morgan, and S. A. Mahmoud, "Resource allocation in cognitive radio-enabled UAV communication," *IEEE Trans. Cogn. Commun. and Netw.*, vol. 8, no. 1, pp. 296–310, 2022.

[6] J. Yuan, Y.-C. Liang, J. Joung, G. Feng, and E. G. Larsson, "Intelligent reflecting surface-assisted cognitive radio system," *IEEE Trans. on Commun.*, vol. 69, no. 1, pp. 675–687, 2021.

[7] L. Zhang, Y. Wang, W. Tao, Z. Jia, T. Song, and C. Pan, "Intelligent reflecting surface aided MIMO cognitive radio systems," *IEEE Trans. Veh. Technol.*, vol. 69, no. 10, pp. 11 445–11 457, 2020.

[8] Y. Wu, F. Zhou, W. Wu, Q. Wu, R. Q. Hu, and K.-K. Wong, "Multi-objective optimization for spectrum and energy efficiency tradeoff in IRS-assisted CRNs with NOMA," *IEEE Trans. Wirel. Commun.*, vol. 21, no. 8, pp. 6627–6642, 2022.

[9] V. N. Vo, N. Q. Long, V.-H. Dang, C. So-In, A.-N. Nguyen, and H. Tran, "Physical layer security in cognitive radio networks for IoT using UAV with reconfigurable intelligent surfaces," in *2021 18th International Joint Conference on Computer Science and Software Engineering (JCSSE)*, 2021, pp. 1–5.

[10] X. Lin, V. Yajnanarayana, S. D. Muruganathan, S. Gao, H. Asplund, H.-L. Maattanen, M. Bergstrom, S. Euler, and Y.-P. E. Wang, "The sky is not the limit: Lte for unmanned aerial vehicles," *IEEE Communications Magazine*, vol. 56, no. 4, pp. 204–210, 2018.

[11] Q. Tao, J. Wang, and C. Zhong, "Performance analysis of intelligent reflecting surface aided communication systems," *IEEE Communications Letters*, vol. 24, no. 11, pp. 2464–2468, 2020.

[12] Q. Wu and R. Zhang, "Intelligent reflecting surface enhanced wireless network via joint active and passive beamforming," *IEEE Trans. Wirel. Commun.*, vol. 18, no. 11, pp. 5394–5409, 2019.

[13] S. Li, B. Duo, M. D. Renzo, M. Tao, and X. Yuan, "Robust secure uav communications with the aid of reconfigurable intelligent surfaces," *IEEE Transactions on Wireless Communications*, vol. 20, no. 10, pp. 6402–6417, 2021.

[14] S. Li, B. Duo, X. Yuan, Y. C. Liang, and M. Renzo, "Reconfigurable intelligent surface assisted UAV communication: Joint trajectory design and passive beamforming," *IEEE Wirel. Commun. Le.*, vol. 9, no. 5, pp. 716–720, 2020.

[15] X. Liu, Y. Yu, F. Li, and T. S. Durrani, "Throughput maximization for RIS-UAV relaying communications," *IEEE Trans. on Intell. Transp. Syst.*, vol. 23, no. 10, pp. 19 569–19 574, 2022.